Journal of Materials Chemistry

Cite this: *J. Mater. Chem.*, 2012, **22**, 9181

www.rsc.org/materials

PAPER

Supramolecular assembly of chiral polyoxometalate complexes for asymmetric catalytic oxidation of thioethers†

Yizhan Wang, Haolong Li, Wei Qi, Yang Yang, Yi Yan, Bao Li and Lixin Wu*

Received 6th December 2011, Accepted 9th March 2012
DOI: 10.1039/c2jm16398e

In this paper, a chiral amphiphilic cation with two stereocenters has been employed to encapsulate a well-known catalytically activated sandwich-type polyoxometalate, $Na_{12}[WZn_3(H_2O)_2(ZnW_9O_{34})_2]$, through electrostatic interaction. The prepared chiral organic cation-encapsulated polyoxometalate complexes were found to self-aggregate into spherical supramolecular assemblies with a diameter of *ca.* 100 nm in the reaction solution. These assemblies, serving as microreactors, exhibited an efficient asymmetric catalytic activity for the oxidation of sulfide with up to 72% enantiomeric excess. The coverage density of chiral organic cations enwrapped on the polyoxometalate surface was proved to have an important influence on the enantioselectivity. Detailed kinetic study of the catalytic process showed that the enantioselectivity of sulfide oxidation was derived from the combination of an ineffective asymmetric sulfoxidation and an effective kinetic resolution of the sulfoxide. The present research strategically offers an understanding for the direct and efficient construction of polyoxometalate based supramolecular catalysts for asymmetric reactions through controlling the surface microenvironment.

Introduction

Asymmetric catalysis continues to be a very attractive area which is related to multidisciplinary sciences due to its importance in both fundamental research and industrial applications. Because of offering a convenient and efficient approach to obtain enantiopure chemicals, the design and construction of new asymmetric catalytic systems with high efficiency has been of great interest in recent years.[1] Polyoxometalates (POMs) are a kind of nano-sized, functional inorganic cluster with abundant compositions and various structures, which have diverse potential applications in catalysis, medicine, and materials science.[2] Due to their specific redox and acidic properties, POMs, as a type of commonly effective catalyst, have been applied for numerous organic transformations, some of which could not be realized or are difficult to be carried out by other known catalysts.[3] However, it is still a big challenge to use POMs for carrying out asymmetric catalysis.[4] Due to the feature of multiple catalytic sites for POMs, it is hard to make all of the sites chirally activated in synthetic chemistry, which greatly decreases the asymmetric products. Meanwhile, the instability and rapid racemization in solution make most POMs with chiral structures lose the activity quickly.[5] To overcome these disadvantages, different synthetic strategies have been devoted to obtaining chiral POM architectures,[4,6] and among of which, a powerful method is to introduce chiral functional groups including organic ligands and metal–organic moieties directly to the surface of POMs *via* covalent bond. Presently, the covalent modified lacunary POMs with novel structures could not provide a very high enantioselectivity.[7] An improved method which couples chiral cations to POM species through electrostatic interaction has been involved recently.[8] The enantioselectivity of enantiopure POMs based on the electrostatic coupling of enantiopure monopodal or tripodal dendritic cations to an achiral $\{PO_4[WO(O_2)_2]_4\}^{3-}$ for asymmetric sulfoxidation was reported. The thioanisole was selectively oxidized to the corresponding chiral sulfoxide with up to 14% enantiomeric excess (ee). Moreover a dendritic effect was noted in the enantioselectivity as the dendritic-POM hybrids are more selective than their non-dendritic counterparts (4% ee). Therefore, understanding the reason of such low enantioselectivity and exploring a general method for the fabrication of asymmetric catalysts based on non-dendritic chiral cations and other common POMs for organic transformations under mild condition are of considerable interest.

Through using hydrophobic tetraalkylammonium cations to substitute the simple counterions, POMs can be transferred to weak polar organic phases.[9] Due to the tight electrostatic interaction, organic cations can cover the surface of a POM polyanion stably, and the substrates can go through the organic layer, performing a homogeneous catalytic process. By changing the organic cations with those having self-assembling capability, we

State Key Laboratory of Supramolecular Structure and Materials, College of Chemistry, Jilin University, Changchun, 130012, P. R. China. E-mail: wulx@jlu.edu.cn; Fax: +86 43185193421; Tel: +86 431 85168481

† Electronic supplementary information (ESI) available: FT-IR, TGA, ^{1}H NMR, UV-vis, and CD data of COEPs; SEM, TEM, DLS and XRD data of the assemblies; ^{1}H NMR and HPLC data of the products. See DOI: 10.1039/c2jm16398e

developed a type of surfactant-encapsulated POM (SEP) complex which possesses a rigid core and a flexible shell. These reverse micelle structure-like hybrid complexes were proved to exhibit versatile self-assembled structures and morphologies in solutions. The most common feature of this system is the tight arrangement of organic cations covering on POMs which locate in the middle of the layered or columnar or tight packed aggregations due to the phase separation of organic and inorganic parts under the driving force of amphiphilicity.[10] Notably, these supramolecular assemblies provide unique locations for modulating the properties of POMs, which would inspire the fabrication of POM-based microreactors, ion-carriers, *etc.*[11] Through immobilization on porous silica matrix, SEPs, as supramolecular catalysts, were confirmed to have high catalytic capacity for the oxidation of sulfides, alcohols and olefins. The hydrophobic interaction between substrates and organic covering around POMs was found to be the important factor to enhance the catalytic performance.[12] Such an understanding was further supported by the results that the microenvironment around POM in SEP assemblies can facilitate the redox reactions and catalytic properties of POMs.[13] We envision that the microenvironment of SEP assemblies could be modified beneficially for asymmetric reactions based on the aforementioned developments and analysis.

Herein, we used a chiral organic cation to encapsulate POM with high catalytic activity through electrostatic interaction, acquiring a chiral organic cation-encapsulated POM (COEP) complex. By employing chiral COEP complexes as building blocks, we successfully constructed the COEP-based supramolecular assemblies bearing abundant stereocenters around the selected POM surface in the reaction system (Scheme 1). The asymmetric oxidation of sulfides, which is meaningful to prepare chiral sulfoxide derivatives in various areas,[14] was chosen as the model reaction to evaluate the enantioselectivity of the COEP assemblies as catalytic microreactors, and up to 72% ee of sulfoxide was obtained in terms of a combined procedure of a less effective asymmetric sulfoxidation and an effective kinetic resolution of the yielded sulfoxide. Considering the facile modification of the chemical microenvironment by choosing various chiral organic cations and POMs, COEP assemblies represent a promising type of supramolecular asymmetric catalyst for diverse asymmetric reactions, which have potentials in fine chemical and biological synthesis.

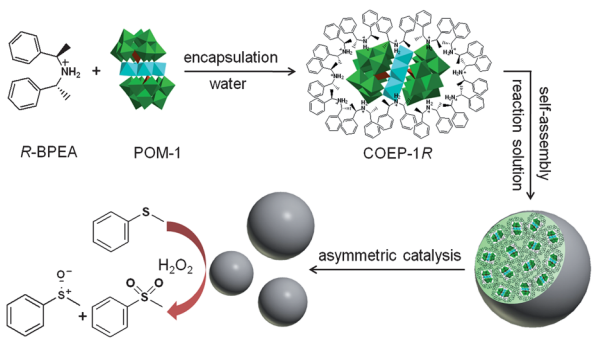

Scheme 1 A schematic illustration of the preparation procedure of COEP-1*R* assemblies and their asymmetric catalytic oxidation for methyl phenyl sulfide with H_2O_2 (30%).

Experimental

Reagents and materials

Hydrogen peroxide (30% aqueous solution) and $H_3PW_{12}O_{40}$ (POM-2) were of analytical grade and purchased from Beijing Chemical Reagents Company. Methyl *p*-tolyl sulfide, bis(1-phenylethyl)amine hydrochloride (*rac*-BPEA), (+)-bis[(*R*)-1-phenylethyl]amine hydrochloride (*R*-BPEA), and (−)-bis[(*S*)-1-phenylethyl]amine hydrochloride (*S*-BPEA) were purchased from Sigma-Aldrich. Benzyl phenyl sulfide, 2-bromophenyl methyl sulfide, 2-chlorophenyl methyl sulfide, and D,L-*sec*-phenethyl alcohol were obtained from J&K Scientific Ltd. Methyl phenyl sulfide, and 2-(methylthio)naphthalene were purchased from Alfa Aesar. All chemicals were used directly without any further purification. All of the solvents used in catalytic reactions were analytical grade. Silica gel (200–300 mesh) was used for column chromatography. $Na_{12}[WZn_3(H_2O)_2(ZnW_9O_{34})_2]\cdot 46H_2O$ (POM-1) and $K_7PW_{11}O_{39}\cdot 12H_2O$ (POM-3) were synthesized according to published procedures.[15]

Measurements

^{1}H NMR spectra were recorded on a Bruker Ultra-Shield TM 500 MHz spectrometer using tetramethlysilane (TMS) as internal standard ($\delta = 0$ ppm). FT-IR spectra were collected on a Bruker Vertex 80v spectrometer equipped with a deuterated triglycine sulfate detector (32 scans) at a resolution of 4 cm^{-1}. The UV-Vis spectra were recorded on a Shimadzu 3100 PC spectrometer. Organic elemental analysis was carried out on a Flash EA1112 from Thermo-Quest Italia S.P.A. Circular dichroism (CD) spectra were carried out on a Bio-Logic MOS-450 spectropolarimeter with a step size of 1 nm and at a speed of 1 nm s^{-1}. Three spectra were recorded and averaged automatically by the instrument. Scanning electron microscope (SEM) images were recorded on a JEOL JSM-6700F field-emission scanning electron microscope. Transmission electron microscopic (TEM) images were obtained with a Hitachi H8100 electron microscope with an accelerating voltage of 200 kV without staining. Dynamic light scattering (DLS) measurements were performed using a Zetasizer NanoZS (Malvern Instruments). Flash chromatography was carried out using 200–300 mesh silica gels. Enantiomeric excess values were determined by HPLC analysis using a SHIMADZU LC-20A equipped with a chiralcel OD-H column (4.6 × 250 mm) obtained from Daicel Chemical Industries, Ltd.

Preparation and characterization of COEPs

COEP-1*R*, *S* and *rac*. The COEP complexes were prepared according to the previously reported procedures,[16] and were confirmed by FT-IR and ^{1}H NMR spectroscopy, elemental analysis, and TG measurements. Taking COEP-1*R* for example: *R*-BPEA (0.1 g, 0.38 mmol) was dissolved in water (20 mL), and an aqueous solution of POM-1 (19.25 mg mL^{-1}, 10 mL) was added with stirring. The initial molar ratio of *R*-BPEA/POM-1 was controlled at about 12 : 1. The mixture was stirred at room temperature for 2 h. Then the yielded precipitate was filtered and washed with deionized water several times until no precipitate was found through treating the filtrate with $AgNO_3$ solution. Then the precipitate was dried under vacuum, giving the complex

COEP-1*R*. The COEP-1*S* and COEP-1*rac* were synthesized by the same procedure. COEP-1*R* (0.13 g) Yield: 54%. ^{1}H NMR (500 MHz, DMSO-d_6, TMS, ppm): δ = 1.36 (6 H, broad), 3.73 (2 H, broad), 7.28–7.38 (10 H, m), 9.29 (2 H, broad). (For *R*-BPEA ^{1}H NMR (500 MHz, DMSO-d_6, TMS, ppm): δ = 1.58 (6 H, d, J = 6.8 Hz), 3.90 (2 H, m), 7.37–7.42 (10 H, m), 10.07 (2 H, broad).) IR (KBr pellet): ν = 3445, 3060, 3032, 2980, 2797, 2496, 1578, 1498, 1454, 1385, 1205, 1070, 924, 877, 764, 700, 542, 441 cm^{-1}. Elemental analysis (%) calcd. for COEP-1*R* ($C_{192}H_{240}N_{12}$ $Zn_5W_{19}O_{68}$, 7623.91): C 30.25, H 3.17, N 2.20; found: C 30.59, H 3.38, N 2.23 (corresponding to the chemical formula: *R*-$BPEA_{12}WZn_3(ZnW_9O_{34})_2$). By assuming that the organic component has decomposed completely and all the inorganic residuals are WO_3 and ZnO at 800 °C the measured residue of 62.7 wt % in total from TGA is in agreement with the calculated value of 63.1 wt % from the given COEP-1*R* formula. COEP-1*S* (0.12 g) Yield: 50%. ^{1}H NMR (500 MHz, DMSO-d_6, TMS, ppm): δ = 1.36 (6 H, broad), 3.73 (2 H, broad), 7.28–7.38 (10 H, m), 9.29 (2 H, broad). IR (KBr pellet): ν = 3429, 3060, 3032, 2980, 2797, 2496, 1578, 1498, 1456, 1384, 1205, 1070, 922, 877, 764, 702, 544, 440 cm^{-1}. Elemental analysis (%) calcd. for COEP-1*S* ($C_{192}H_{240}N_{12}$ $Zn_5W_{19}O_{68}$, 7623.91): C 30.25, H 3.17, N 2.20; found: C 30.83, H 3.39, N 2.29 (corresponding to the chemical formula: *S*-$BPEA_{12}WZn_3(ZnW_9O_{34})_2$). COEP-1*rac* (0.11 g) Yield: 46%. ^{1}H NMR (500 MHz, DMSO-d_6, TMS, ppm): δ = 1.36 (6 H, broad), 3.73 (2 H, broad), 7.28–7.38 (10 H, m), 9.29 (2 H, broad). IR (KBr pellet): ν = 3425, 3060, 3032, 2974, 2793, 2490, 1580, 1498, 1456, 1383, 1205, 1076, 922, 877, 764, 700, 542, 441 cm^{-1}. Elemental analysis (%) calcd. for COEP-1*rac* ($C_{192}H_{240}N_{12}$ $Zn_5W_{19}O_{68}$, 7623.91): C 30.25, H 3.17, N 2.20; found: C 30.49, H 3.14, N 2.15 (corresponding to the chemical formula: *rac*-$BPEA_{12}WZn_3(ZnW_9O_{34})_2$).

COEP-2*R*. *R*-BPEA (0.2 g, 0.76 mmol) was dissolved in water (30 mL), and an aqueous solution of POM-2 (24.33 mg mL^{-1}, 30 mL) was added with stirring. The initial molar ratio of *R*-BPEA/POM-2 was controlled at about 3 : 1. After the mixture was stirred at room temperature for 2 h, the formed precipitate was filtered and washed with deionized water (30 mL) 3 times and dried under vacuum, giving the complex COEP-2*R* (0.81 g). Yield: 90%. IR (KBr pellet): ν = 3070, 3037, 2983, 2798, 2478, 1578, 1497, 1458, 1385, 1080, 976, 895, 812, 764, 698, 541, 442 cm^{-1}. Elemental analysis (%) calcd. for COEP-2*R* ($C_{48}H_{60}N_3PW_{12}O_{40}$, 3556.04): C 16.21, H 1.70, N 1.18; found: C 16.58, H 1.85, N 1.26 (corresponding to the chemical formula: R-$BPEA_3PW_{12}O_{40}$).

COEP-3*R*. *R*-BPEA (0.2 g, 0.76 mmol) was dissolved in water (30 mL), and an aqueous solution of POM-3 (11.52 mg mL^{-1}, 30 mL) was added with stirring. The initial molar ratio of *R*-BPEA/POM-3 was controlled at about 7 : 1. After the mixture was stirred at room temperature for 2 h, the formed precipitate was filtered and washed with deionized water (30 mL) 3 times and dried under vacuum, giving the predicted complex COEP-3*R* (0.3 g). Yield: 60%. IR (KBr pellet): ν = 3447, 3060, 3032, 2980, 2796, 2496, 1608, 1580, 1498, 1456, 1385, 1205, 1072, 1045, 945, 876, 852, 808, 762, 700, 542, 513 cm^{-1}. Elemental analysis (%) calcd. for COEP-3*R* ($C_{96}H_{120}N_6KPW_{11}O_{39}$, 4074.30): C 28.29, H 2.97, N 2.06; found: C 28.20, H 3.32, N 1.68 (corresponding to the chemical formula: *R*-$BPEA_6KPW_{11}O_{39}$).

Typical catalytic procedure for asymmetric oxidation of sulfide

To a 10 mL round bottom flask was added COEP-1*R* (0.4 μmol) and methyl phenyl sulfide (0.4 mmol) in $CHCl_3$ (2 mL). When the mixture was cooled to 0 °C, 30% H_2O_2 (2 equiv.) was added, and stirred (500 r min^{-1}) at that temperature for a certain period of time. The reaction progress was monitored by TLC and HPLC. After the reaction, the catalyst was precipitated by the addition of diethyl ether, and the solid was filtered and washed with diethyl ether two times, giving the recovered catalyst. The filtrate was evaporated under reduced pressure, and the residue was purified by flash chromatography on silica gel to isolate the desired product (cyclohexane/ethyl acetate 1 : 1; v/v as eluent). The enantiomeric excess was determined by chiral HPLC on a chiralcel OD-H column and detected by UV detector (254 nm) at 30 °C through eluting with hexane/isopropanol (90 : 10) at a flow rate of 1 mL min^{-1}. The catalytic reaction system is safe under the reaction conditions. The safety concerning the phosgene formation in the mixture solution of $CHCl_3$ and 30% H_2O_2 under the catalytic condition is dealt with in the ESI.†

Reaction procedure for kinetic resolution of sulfoxides

COEP-1*R* or COEP-1*S* (0.4 μmol) and racemic methyl phenyl sulfoxide (0.4 mmol) were dissolved in chloroform (2 mL) in a 10 mL round bottom flask, then the mixture was cooled to 0 °C, and H_2O_2 (1 equiv. 30%) was added under stirring (500 r min^{-1}) at this temperature. During the reaction process, a certain amount of the reaction mixture was taken out and monitored by TLC and HPLC at an appropriate time interval. When the reaction was completed, the catalyst was precipitated by the addition of diethyl ether and the solid was filtered, washed with diethyl ether two times and recovered. The filtrate was evaporated under reduced pressure, and the residue was purified by flash chromatography on silica gel to isolate the desired product (cyclohexane/ethyl acetate 1 : 1; v/v as eluent). The ee value was determined by chiral HPLC on a chiralcel OD-H column through eluting with hexane/isopropanol (90 : 10) at a flow rate of 1 mL min^{-1} at 30 °C using a UV detector (254 nm).

Typical catalytic procedure for the kinetic resolution of secondary alcohol

D,L-*sec*-phenethyl alcohol (0.4 mmol) and 30% H_2O_2 (1 equiv.) were added in $CHCl_3$ (2 mL) to a 10 mL round bottom flask. Then COEP-1*R* (0.4 μmol) was added. The reaction mixture was stirred with a speed of 500 r min^{-1} at 70 °C and the progress of the reaction was monitored by TLC and ^{1}H NMR. After the reaction was completed, the catalyst was precipitated by adding diethyl ether, and the solid was filtered. The filtrate was evaporated under reduced pressure, and the residue was purified by flash chromatography on silica gel to isolate the desired product (dichloromethane as eluent). 4% ee of the remaining 1-phenylethanol was produced with a 36% conversion of phenethyl alcohol. The ee value was determined by chiral HPLC on a chiralcel OD-H column, eluting with hexane/isopropanol (95 : 5) at a flow rate of 1 mL min^{-1} through a UV detector (254 nm) at 30 °C.

Results and discussion

Preparation and characterization of COEPs

To construct a high efficient POM-based catalyst, a known catalytically active sandwich type POM, $Na_{12}[WZn_3(H_2O)_2(ZnW_9O_{34})_2]\cdot 46H_2O$ (POM-1),[17] was chosen for the present purpose. We selected commercially available chiral cationic ammoniums with two stereocenters, (+)-bis[(*R*)-1-phenylethyl]amine hydrochloride (*R*-BPEA) and (−)-bis[(*S*)-1-phenylethyl]amine hydrochloride (*S*-BPEA), to encapsulate the POM through the ion substitution reaction, obtaining two complexes COEP-1*R* and COEP-1*S*. The complex COEP-1*rac*, using racemic bis(1-phenylethyl)amine hydrochloride (*rac*-BPEA), was also prepared to perform a control experiment. In contrast to POM-1, which is soluble in water, all of the COEPs are immiscible in water but readily dissolve in organic media such as dichloromethane, acetonitrile and dimethyl sulfoxide, suggesting that POM-1 has been successfully given a hydrophobic covering due to the charge neutralization. The characteristic vibrational bands at around 924, 877, and 764 cm^{-1} were found in IR spectra of these COEPs (Fig. S1†), as observed for bare POM-1, confirming the well retained framework structure of POM-1 after the encapsulation. Meanwhile, as shown in the UV-Vis spectra, the appearance of an absorption band at around 256 nm for the benzene ring in COEP-1*R* indicates that the counterions of POM-1 are replaced by chiral organic cations (Figs S2–3†). There are no obvious differences in the IR and UV spectra among COEP-1*R*, COEP-1*rac*, and COEP-1*S*. The elemental analysis and thermogravimetric analysis demonstrate that all the counterions of POM-1 have been replaced by chiral cations and the structural formulae of all of the three COEPs can be anticipated as $(C_{16}H_{20}N)_{12}WZn_3(ZnW_9O_{34})_2$ (Fig. S4†). Comparing the ^{1}H NMR spectra of COEP-1*R* with the corresponding organic cation, we find that the ^{1}H signal of the N–H group of COEP-1*R* shifts from 10.07 to 9.29 ppm and the signal of the proton on the chiral carbon moves from 3.90 to 3.73 ppm while the signal of the $-CH_3$ group shifts from 1.58 to 1.36 ppm (Fig. 1). All these signals of the three COEPs have moved to the higher field and become broadened (Fig. S5†), which confirms the existence of electrostatic interactions between the organic cation and POM-1.[18]

The chiroptical activity of COEPs has been investigated using circular dichroism (CD) spectroscopy in acetonitrile and in dichloromethane. As expected, COEP-1*R* and COEP-1*S* show mirror-symmetric CD spectra in acetonitrile, in contrast to a lack of signal for COEP-1*rac* (Fig. S6†), demonstrating the enantiopurity of the two COEPs (Fig. 2). The Cotton effects appearing at around 193 and 218 nm are comparable with the corresponding bands of the organic ammonium cation at almost the same wavelengths. The chiroptical activity of COEP-1*R* and COEP-1*S* indicates that the chirality of the chiral organic cations is maintained during the encapsulation process. A mirror symmetric CD signal at around 280 nm which was observed in the spectra of COEP-1*R* and COEP-1*S* can be ascribed to the O → W charge-transfer band of POM-1.[7,8] Similar chiroptical properties of these complexes were also observed in dichloromethane.

To evaluate the asymmetric catalytic activity dependence of COEPs on the stereocenter coverage density, here, we define the stereocenter coverage density as the number of stereocenters per POM surface area. We used *R*-BPEA to encapsulate two POMs with less surface charge density, $H_3PW_{12}O_{40}$ (POM-2) and $K_7PW_{11}O_{39}\cdot 12H_2O$ (POM-3), respectively. The obtained complexes $(C_{16}H_{20}N)_3PW_{12}O_{40}$ (COEP-2*R*) and $(C_{16}H_{20}N)_6KPW_{11}O_{39}$ (COEP-3*R*), are characterized (Figs S7–8†) and they exhibit similar CD spectral properties to chiral organic cations.

Self-assembly of COEPs

The self-assembly behaviour of SEPs in the reaction system can affect the microenvironment of POMs and improve their catalytic efficiency. Interestingly, the present COEPs bearing rigid benzyl rings, rather than long alkyl chains, also show obvious self-assembly behaviours under the reaction conditions. We studied the property of COEP-1*R* under the reaction conditions used for asymmetric catalytic oxidation of methyl phenyl sulfide. The oxidation of prochiral methyl phenyl sulfide to the corresponding sulfoxide with hydrogen peroxide (30%) in a biphasic mixture of water and chloroform was carried out by using

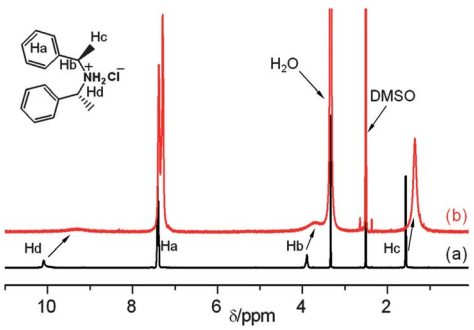

Fig. 1 ^{1}H NMR spectra of (a) *R*-BPEA and (b) COEP-1*R* in DMSO-d_6.

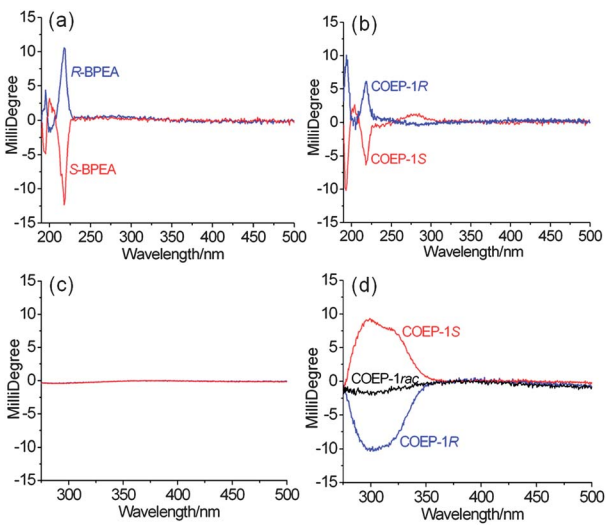

Fig. 2 CD spectra of *R*-BPEA and *S*-BPEA (a) in CH_3CN at $c = 3 \times 10^{-4}$ mol L^{-1}, and (c) in CH_2Cl_2 at $c = 1.5 \times 10^{-3}$ mol L^{-1}; CD spectra of COEP-1*R* and COEP-1*S* (b) in CH_3CN at $c = 2.6 \times 10^{-5}$ mol L^{-1}, and (d) in CH_2Cl_2 at $c = 1.3 \times 10^{-4}$ mol L^{-1}.

COEP-1*R* as the catalyst at room temperature. An obvious Tyndall scattering suggests that the self-assembly of COEP-1*R* occurs in the reaction solution (Fig. S9†). The dynamic light scattering (DLS) result gives a hydrodynamic diameter of *ca.* 106 nm for the size of the assemblies (Fig. 3). In contrast, before the hydrogen peroxide solution was added into the reaction solution, COEP-1*R* was found in a monodispersed state as the measured hydrodynamic diameter is only 4.2 nm, very small and close to the size scale of a single COEP-1*R* complex and no Tyndall phenomenon can be observed.

The self-assembly behaviours of COEP-1*R* were further confirmed by TEM and SEM measurements (Fig. 4 and Fig. S10†). Upon the addition of hydrogen peroxide solution, large assemblies of COEP-1*R* with a regular spherical shape form immediately in an average diameter of *ca.* 100 nm, which is consistent with the DLS results (Fig. 4). However, COEP-1*R* alone does not show obvious aggregation in the reaction solution without the addition of hydrogen peroxide solution, as demonstrated by TEM, shown in Fig. S10†. Therefore, one can conclude that COEP-1*R* undergoes a self-assembly process in the reaction solution following the addition of polar hydrogen peroxide and a spherical nanostructure forms *in situ* at the beginning of the reaction. The polar hydrogen peroxide solution not only plays a role as an oxidant, but also serves as an inducer for assemblies. It is known that the polarity of the solvent can modulate the assembled state of SEPs.[10b] When the hydrogen peroxide solution is added, the polarity of the reaction solution increases due to the dissolution of a small amount of hydrogen peroxide solution. Thus, the increased polarity of the reaction solution drives COEP-1*R* to form self-assemblies due to the increased hydrophobic interaction and Van der Waals force.[19] The broad reflection peak at *ca.* 4.5° in the X-ray diffraction result (Fig. S11†) confirms that the COEP-1*R* just aggregates into a tight packed assembly with non-ordered structure. The observed self-assemblies are favourable for improving the chiral microenvironment around the POMs. The tight packing fixes chiral groups stiffly and increases the coverage density of the stereocenter on the POM surface in the assemblies. The assemblies are proved to be quite stable, and maintain the aggregation morphology even after the reaction (Fig. 4d). The DLS result confirms the assemblies remaining in a hydrodynamic diameter of *ca.* 122 nm in the solution after the reaction has finished (Fig. S12†). Identically, COEP-1*S* and COEP-1*rac* in the reaction solution exhibit the same self-assembly properties as those of COEP-1*R*.

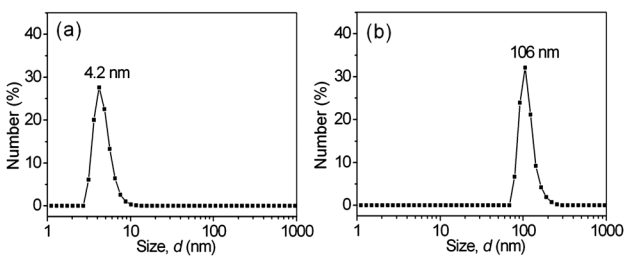

Fig. 3 DLS plots of COEP-1*R* (0.4 μmol) in the reaction system for methyl phenyl sulfide (0.4 mmol) oxidation in $CHCl_3$ (2 mL) (a) without and (b) with addition of H_2O_2 (30%, 0.4 mmol) at room temperature.

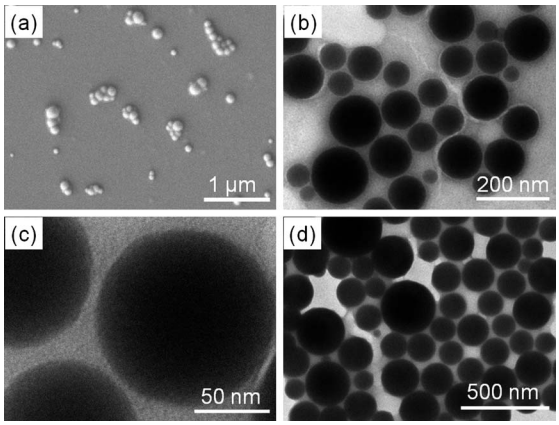

Fig. 4 (a) SEM and (b–d) TEM images of COEP-1*R* (0.4 μmol) in $CHCl_3$ (2 mL) containing methyl phenyl sulfide (0.4 mmol) and H_2O_2 (30%, 0.4 mmol) at room temperature, where (a) and (b) are at the beginning, (d) is after the reaction finished and (c) is the amplified image of (b).

Meanwhile, regular spherical assemblies were also observed for COEP-3*R* in the reaction solution of methyl phenyl sulfide oxidation in chloroform (Fig. S13†). However, due to the poor solubility, we could not study the self-assembly behaviours of COEP-2*R* in the reaction solution.

Catalytic activity of COEPs

The asymmetric catalytic activities of COEP-1*R* assemblies in the oxidation of prochiral methyl phenyl sulfide under different conditions were listed in Table 1. Due to the temperature-dependent rotational disorder of chiral groups, we decreased the reaction temperature to 0 °C and obtained a bit higher enantioselectivity in 18% ee than at room temperature in chloroform (Table 1, entries 1 and 2), while the self-assembly behaviour of COEP-1*R* remained the same at this temperature. Importantly, the solvents employed in the catalytic reaction were found to have remarkable effects on the ee value and the conversion. In dichloromethane with a similar polarity to that of chloroform, COEP-1*R* also forms stable assemblies and the enantioselectivity (14% ee) is close to that in chloroform. In acetonitrile, where the polarity is higher than chloroform, we did not observe stable assemblies (Fig. S14†), and the enantioselectivity became very low (1% ee). Due to the poor solubility of COEP-1*R* in hexane, the unfavorable mass transfer makes the catalytic reaction suppressed. Interestingly, the enantioselectivity can increase greatly by an overoxidation of the resultant sulfoxide through a kinetic resolution process. Upon raising the amount of hydrogen peroxide from 1 to 2 equiv. (Table 1, entry 6), the reaction accelerates quite a lot and the yield for sulfoxide reduces from 81.6 to 64% within the same reaction time due to the increased overoxidation to the sulfone, while the ee value raises from 18 to 25%. An increase of the reaction time from 6 to 10 h raises the ee value from 25 to 40%, while the amount of sulfone increases from 36 to 64%. Further prolonging the reaction time up to 17 h yields a 72% ee and 95% sulfone simultaneously.

To confirm the dependence of the enantioselectivity on the coverage density of the stereocenter on the POM surface, we

Table 1 A summary of the asymmetric catalytic activity of COEP-1*R* for the oxidation of methyl phenyl sulfide with 30% H_2O_2 under different conditions[a]

Entry	Catalyst	Solvent	*t* (h)	H_2O_2 (equiv.)	Conv. (%)[b]	SO : SO_2 (%)[c]	ee (%)[d]
1	COEP-1*R*	$CHCl_3$	6	1	88	85 : 15	6 (*R*)
2	COEP-1*R*	$CHCl_3$	6	1	85	96 : 4	18 (*R*)
3	COEP-1*R*	CH_2Cl_2	6	1	79	95 : 5	14 (*R*)
4	COEP-1*R*	CH_3CN	6	1	55	95 : 5	1 (*R*)
5	COEP-1*R*	hexane	6	1	<1	—	—
6	COEP-1*R*	$CHCl_3$	6	2	100	64 : 36	25 (*R*)
7	COEP-1*R*	$CHCl_3$	10	2	100	36 : 64	40 (*R*)
8	COEP-1*R*	$CHCl_3$	17	2	100	5 : 95	72 (*R*)
9	COEP-2*R*	$CHCl_3$	10	1	5	100 : 0	1 (*R*)
10	COEP-3*R*	$CHCl_3$	6	1	78	95 : 5	5 (*R*)
11	*R*-BPEA	$CHCl_3$	10	2	—	—	—
12	COEP-1*rac*	$CHCl_3$	10	2	100	35 : 65	0
13	COEP-1*rac*	$CHCl_3$	17	2	100	3 : 97	0
14	COEP-1*S*	$CHCl_3$	10	2	100	40 : 60	43 (*S*)

[a] All reactions are performed with sulfide (0.4 mmol) and catalysts (0.4 μmol) in different solvents (2 mL) at 0 °C except entry 1, which is at room temperature. [b] The conversions are determined by HPLC based on the crude reaction mixture. [c] SO and SO_2 stand for sulfoxide and sulfone, respectively. [d] ee values are measured by HPLC analysis with a chiralcel OD-H column, and the absolute configuration is determined by comparison of the HPLC results with the data in the literature.[21]

evaluated the catalytic reactions of COEP-2*R* and COEP-3*R* (Table 1, entries 9 and 10) under similar reaction conditions to those for catalysis by COEP-1*R*. The densities of the stereocenter per surface area on the POMs are 6/S, 12/S, and *ca.* 14/S for COEP-2*R*, COEP-3*R* and COEP-1*R*, respectively (Table S1†). Interestingly, with the coverage density of the stereocenter decreasing, the enantioselectivity of methyl phenyl sulfide asymmetric oxidation decreases dramatically. The increase of stereocenter coverage density can make more chiral groups surround the POM surface, leading to a higher efficiency of chiral inducement. Increasing the surface charge density of POMs could make the corresponding COEP have a higher coverage density of stereocenters. Comparing with the monodispersed complexes, the close packed nanostructure of the aggregated complexes will certainly drive the increase of the stereocenter coverage density on the POM surface. Therefore, the complex structure and the self-assembly structure may both have an influence on the enantioselectivity of the reaction system.

A synergetic catalysis between the chiral organic cations and POMs, driven by electrostatic interaction, was found to exist in the COEP complexes. When COEP-1*R* performs as a catalyst, the absolute configuration of sulfoxide is *R*, and when COEP-1*S* is used as catalyst, the absolute configuration of sulfoxide is *S*. At the same reaction time, the two reactions present comparable ee values (40% *versus* 43% ee) (Table 1, entries 7 and 14). As expected, when the COEP-1*rac* is used, the product is racemic (Table 1, entries 12 and 13). Additionally, when using the chiral cation *R*-BPEA rather than COEP complexes as the catalyst, the reaction does not proceed at all, indicating that the reaction is catalyzed by the POM part. Therefore, we infer that the chirality of sulfoxide is originated from the asymmetric induction of chiral cations. POM-1 anionic cluster and chiral organic cations incorporated in the COEP unit show a synergistic effect in the self-assemblies, where the chiral cations provide an asymmetric microenvironment and the POMs contribute to the catalysis of oxidation.

A kinetic study was carried out to track the course of the asymmetric reaction (Fig. 5a). The kinetic profile for the oxidation of methyl phenyl sulfide in the presence of 2.5 equiv. hydrogen peroxide illustrates the dependence of the ee value of sulfoxide on the relative concentrations of sulfone. A 10% ee value is obtained at the initial stage of the reaction, which is improved to 70% ee with 95% sulfone after 12 h of reaction. This fact indicates that two consecutive reactions are taking place, one is the asymmetric oxidation of sulfide to sulfoxide and the other is the subsequent kinetic resolution through yielding sulfone. In the two independent enantioselective processes, the ee value of the sulfoxide increases steadily, which implies that both the processes co-contribute to the same enantiomer. The concentration of sulfoxide reaches a maximum

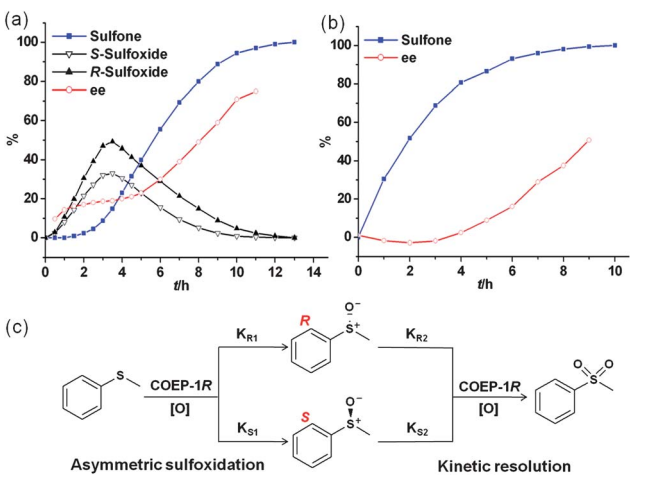

Fig. 5 Time profiles of the oxidation of (a) methyl phenyl sulfide (0.4 mmol) with H_2O_2 (30%, 1.0 mmol), (b) racemic methyl phenyl sulfoxide (0.4 mmol) with H_2O_2 (30%, 0.4 mmol) using COEP-1*R* (0.4 μmol) as an asymmetric catalyst in $CHCl_3$ (2 mL) at 0 °C; and (c) the asymmetric sulfoxidation and kinetic resolution process for the oxidation reaction of methyl phenyl sulfide.

in 3 h. Before the critical moment, the asymmetric sulfoxidation is the main process, in which the formation rate of *S*-sulfoxide is slower than that of *R*-sulfoxide ($K_{R1} > K_{S1}$) and only 20% ee can be obtained. After the moment, a main process with more efficient kinetic resolution follows, in which the rate of *S*-sulfoxide transferring into sulfone is faster than *R*-sulfoxide ($K_{R2} < K_{S2}$) and thus the ee value of *R*-sulfoxide raises up to 70%. Precedents for such a sequence in which the asymmetric sulfoxidation is followed by sulfoxide kinetic resolution have been reported in the literature.[20] To confirm the contribution of kinetic resolution to the enantioselectivity, the catalytic oxidation of racemic methyl phenyl sulfoxide was performed with COEP-1*R*. More *S*-sulfoxide was oxidized to sulfone, which directly supports that the kinetic resolution produces the excess *R* enantiomer. From the kinetic profile (Fig. 5b), the ee value of *R*-sulfoxide firstly undergoes a platform stage and then, the ee value increases steadily with the reaction time getting longer. When the kinetic resolution of racemic sulfoxide was performed with COEP-1*S*, opposite to the reaction with COEP-1*R*, more *R*-sulfoxide was oxidized to sulfone leaving *S*-sulfoxide as the main product at last. Similarly, the ee value of *S*-sulfoxide firstly undergoes a platform stage and then, the ee value increases steadily with the reaction time getting longer (Fig. S15†).

Under the optimized reaction conditions, the present catalytic system can be expanded to other sulfide derivatives, and the results were listed in Table 2. By using COEP-1*R* as the catalyst, optically active products of the relevant alkyl aryl sulfides are obtained. The ee values of 2-(methylsulfinyl)naphthalene and methyl *p*-tolyl sulfoxide depend on the amount of overoxidation to the corresponding sulfone. When the methyl group is replaced by a benzyl group, 51% ee can be obtained with 75% of sulfone formation. We also evaluated the enantioselectivity for the oxidation of *ortho*-substituted alkyl–aryl sulfides (Table 2 entries 7–10). For 2-bromophenyl methyl sulfide, 25% ee can be obtained with 99% of sulfoxide formation within 8 h. Further prolonging the reaction time, only a small amount of sulfoxide is overoxidized to sulfone with a small improvement in the ee value. Similar results are obtained for 2-chlorophenyl methyl sulfide. For all the substrates, to get a higher ee value, a larger amount of sulfone is unavoidable, which further demonstrates that the enantioselectivity is sourced from the combination of asymmetric sulfide oxidation and the kinetic resolution by the overoxidation of the resultant sulfoxide.

Notably, the COEPs possess a practical feature as catalysts because they can be reused after a simple recovery process through precipitation with diethyl ether. Three catalytic cycles were carried out and only a slight loss in activity, chemoselectivity, and enantioselectivity was found (Table S2†). The IR spectrum of the recovered catalyst shows similar peaks to the original one, suggesting that the structure of POM-1 is well maintained after the catalytic reaction (Fig. S16†). Although the catalytic reaction mechanism is not clear, we believe that H_2O_2 firstly reacts with POM to form activated POM, which subsequently oxidizes the substrates in the chiral environment and returns to the original POM state.[17] Finally, to demonstrate the catalytic generality of COEPs for other types of asymmetric oxidation reactions, we evaluated the asymmetric catalytic activities for the kinetic resolution of racemic 1-phenylethanol with COEP-1*R*. Though the ee value was quite low (4% ee), the obvious catalytic activity of the chiral complex suggests COEPs are promising asymmetric catalysts for various reactions based on POMs.

Conclusions

In conclusion, COEPs can self-assemble into well defined spherical assemblies in the reaction solutions, which act as microreactors for asymmetric sulfoxidation. The synergistic effect predominates the catalytic process, in which the POM contributes to the catalysis of sulfoxidation and the chiral organic part provides a chiral microenvironment. The coverage density of the chiral component on the POM surface has been proved to be involved in the enantioselectivity. The self-assemblies enhance the coverage density of chiral organic cations surrounding POMs, providing an efficient microenvironment for chiral inducement through a combined procedure of a less effective asymmetric sulfoxidation and an effective kinetic resolution of the yielded sulfoxide. In addition to the sulfide derivatives, other catalytic oxidation reactions could also be performed with this type of supramolecular catalysts. Following the current understanding, the present study offers a strategically universal protocol for the direct and efficient construction of more selective and robust supramolecular asymmetric catalysts

Table 2 A summary of the asymmetric catalytic activity of COEP-1*R* for the oxidation of different sulfides[a]

Entry	Substrates	*t* (h)	Conv. (%)	SO : SO_2 (%)[b]	ee (%)[c]
1	2-(methylthio)naphthalene	10	100	56 : 44	30 (*R*)
2	2-(methylthio)naphthalene	14	100	34 : 66	35 (*R*)
3	Methyl *p*-tolyl sulfide	11	100	30 : 70	33 (*R*)
4	Methyl *p*-tolyl sulfide	17	100	10 : 90	53 (*R*)
5	Benzyl phenyl sulfide	5	100	76 : 24	22 (*R*)
6	Benzyl phenyl sulfide	12	100	25 : 75	51 (*R*)
7	2-bromophenyl methyl sulfide	8	100	99 : 1	25
8	2-bromophenyl methyl sulfide	24	100	95 : 5	27
9	2-chlorophenyl methyl sulfide	6	100	97 : 3	22
10	2-chlorophenyl methyl sulfide	24	100	91 : 9	24

[a] All reactions are performed with sulfides (0.4 mmol), H_2O_2 (30%, 0.8 mmol), and COEP-1*R* (0.4 μmol) in $CHCl_3$ (2 mL) at 0 °C. [b] SO and SO_2 stand for sulfoxide and sulfone respectively. [c] The ee values are measured by HPLC analysis with a chiralcel OD-H column, and the absolute configuration is determined by comparison of the HPLC results with the data in the literature.[21]

based on POMs, which is important for potential applications in asymmetric synthesis.

Acknowledgements

The authors acknowledge the financial support from National Basic Research Program (2007CB808003), National Natural Science Foundation of China (20973082, 20921003), 111 Project (B06009) for supporting the fruitful discussion with Prof. N. M. at University of Tokyo, and Open Project from SKL of Polymer Physics and Chemistry, CIAC.

Notes and references

1 I. Ojima, *Catalytic Asymmetric Synthesis*, Wiley-VCH, 3rd Edition, 2010.
2 (*a*) M. T. Pope and A. Müller, *Angew. Chem., Int. Ed. Engl.*, 1991, **30**, 34; (*b*) special issue on "polyoxometalates", *Chem. Rev.*, 1998, **98**, 1; (*c*) A. Proust, R. Thouvenot and P. Gouzerh, *Chem. Commun.*, 2008, 1837; (*d*) D. L. Long, R. Tsunashima and L. Cronin, *Angew. Chem. Int. Ed.*, 2010, **49**, 1736; (*e*) F. Li and L. Xu, *Dalton Trans.*, 2011, **40**, 4024; (*f*) B. Keita, T. Liu and L. Nadjo, *J. Mater. Chem.*, 2009, **19**, 19; (*g*) Z. Wang, R. Zhang, Y. Ma, A. Peng, H. Fu and J. Yao, *J. Mater. Chem.*, 2010, **20**, 271; (*h*) Z. Wang, Y. Ma, R. Zhang, A. Peng, Q. Liao, Z. Cao, H. Fu and J. Yao, *Adv. Mater.*, 2009, **21**, 1737; (*i*) S. Li, X. Yu, G. Zhang, Y. Ma, J. Yao, B. Keita, N. Louis and H. Zhao, *J. Mater. Chem.*, 2011, **21**, 2282.
3 (*a*) I. A. Weinstock, E. M. G. Barbuzzi, M. W. Wemple, J. J. Cowan, R. S. Reiner, D. M. Sonnen, R. A. Heintz, J. S. Bond and C. L. Hill, *Nature*, 2001, **414**, 191; (*b*) I. V. Kozhevnikov, *Chem. Rev.*, 1998, **98**, 171; (*c*) K. Kamata, T. Hirano, R. Ishimotoa and N. Mizuno, *Dalton Trans.*, 2010, **39**, 5509; (*d*) K. Kamata, K. Yonehara, Y. Sumida, K. Yamaguchi, S. Hikichi and N. Mizuno, *Science*, 2003, **300**, 964; (*e*) Z. Xi, N. Zhou, Y. Sun and K. Li, *Science*, 2001, **292**, 1139; (*f*) G. S. Armatas, G. Bilis and M. Louloudi, *J. Mater. Chem.*, 2011, **21**, 2997; (*g*) G. S. Armatas, A. P. Katsoulidis, D. E. Petrakis and P. J. Pomonis, *J. Mater. Chem.*, 2010, **20**, 8631.
4 B. Hasenknopf, K. Micoine, E. Lacôte, S. Thorimbert, M. Malacria and R. Thouvenot, *Eur. J. Inorg. Chem.*, 2008, 5001, and references cited therein.
5 X. K. Fang, T. M. Anderson and C. L. Hill, *Angew. Chem., Int. Ed.*, 2005, **44**, 3540.
6 (*a*) H. An, E. Wang, D. Xiao, Y. Li, Z. Su and L. Xu, *Angew. Chem., Int. Ed.*, 2006, **45**, 904; (*b*) U. Kortz, M. G. Savelieff, F. Y. A. Ghali, L. M. Khalil, S. A. Maalouf and D. I. Sinno, *Angew. Chem., Int. Ed.*, 2002, **41**, 4070; (*c*) X. Fang, T. M. Anderson, Y. Hou and C. L. Hill, *Chem. Commun.*, 2005, 5044; (*d*) M. Lu, J. H. Kang, D. G. Wang and Z. H. Peng, *Inorg. Chem.*, 2005, **44**, 7711; (*e*) M. Carraro, A. Sartorel, G. Scorrano, C. Maccato, M. H. Dickman, U. Kortz and M. Bonchio, *Angew. Chem., Int. Ed.*, 2008, **47**, 7275; (*f*) H. Naruke, J. Iijima and T. Sanji, *Inorg. Chem.*, 2011, **50**, 7535; (*g*) K. Micoine, B. Hasenknopf, S. Thorimbert, E. Lacôte and M. Malacria, *Angew. Chem., Int. Ed.*, 2009, **48**, 3466.
7 M. Carraro, G. Modugno, A. Sartorel, G. Scorrano and M. Bonchio, *Eur. J. Inorg. Chem.*, 2009, 5164.
8 (*a*) C. Jahier, M. Cantuel, N. D. McClenaghan, T. Buffeteau, D. Cavagnat, F. Agbossou, M. Carraro, M. Bonchio and S. Nlate, *Chem.–Eur. J.*, 2009, **15**, 8703; (*b*) C. Jahier, M.-F. Coustou, M. Cantuel, N. D. McClenaghan, T. Buffeteau, D. Cavagnat, M. Carraro and S. Nlate, *Eur. J. Inorg. Chem.*, 2011, 727.
9 C. Venturello and R. D'Aloisio, *J. Org. Chem.*, 1988, **53**, 1553.
10 (*a*) H. Wang, Y. Yan, B. Li, L. Bi and L. Wu, *Chem.–Eur. J.*, 2011, **17**, 4273; (*b*) H. Li, H. Sun, W. Qi, M. Xu and L. Wu, *Angew. Chem., Int. Ed.*, 2007, **46**, 1300; (*c*) Y. Yang, Y. Wang, H. Li, W. Li and L. Wu, *Chem.–Eur. J.*, 2010, **16**, 8062; (*d*) Y. Yan, B. Li, W. Li, H. Li and L. Wu, *Soft Matter*, 2009, **5**, 4047; (*e*) Y. Yan, H. Wang, B. Li, G. Hou, Z. Yin, L. Wu and V. W. W. Yam, *Angew. Chem., Int. Ed.*, 2010, **49**, 9233; (*f*) D.-L. Long, E. Burkholder and L. Cronin, *Chem. Soc. Rev.*, 2007, **36**, 105; (*g*) J. Zhang, Y.-F. Song, L. Cronin and T. Liu, *J. Am. Chem. Soc.*, 2008, **130**, 14408.
11 (*a*) H. Li, Y. Yang, Y. Wang, W. Li, L. Bi and L. Wu, *Chem. Commun.*, 2010, **46**, 3750; (*b*) H. Li, Y. Yang, Y. Wang, C. Wang, W. Li and L. Wu, *Soft Matter*, 2011, **7**, 2668.
12 W. Qi, Y. Wang, W. Li and L. Wu, *Chem.–Eur. J.*, 2010, **16**, 1068.
13 (*a*) A. Nisar, Y. Lu, J. Zhuang and X. Wang, *Angew. Chem., Int. Ed.*, 2011, **50**, 3187; (*b*) A. Nisar, J. Zhuang and X. Wang, *Adv. Mater.*, 2011, **23**, 1130.
14 (*a*) I. Fernández and N. Khiar, *Chem. Rev.*, 2003, **103**, 3651; (*b*) E. Wojaczyńska and J. Wojaczyński, *Chem. Rev.*, 2010, **110**, 4303; (*c*) M. C. Carreño, G. Hernández-Torres, M. Ribagorda and A. Urbano, *Chem. Commun.*, 2009, 6129.
15 (*a*) C. M. Tourné, G. F. Tourné and F. Zonnevijlle, *J. Chem. Soc., Dalton Trans.*, 1991, 143; (*b*) N. Haraguchi, Y. Okaue, T. Isobe and Y. Matsuda, *Inorg. Chem.*, 1994, **33**, 1015.
16 W. Qi, H. Li and L. Wu, *Adv. Mater.*, 2007, **19**, 1983.
17 (*a*) R. Neumann and M. Gara, *J. Am. Chem. Soc.*, 1995, **117**, 5066; (*b*) W. Adam, P. L. Alsters, R. Neumann, C. R. Saha-Möller, D. Sloboda-Rozner and R. Zhang, *Synlett*, 2002, **12**, 2011; (*c*) W. Adam, P. L. Alsters, R. Neumann, C. R. Saha-Möller, D. Sloboda-Rozner and R. Zhang, *J. Org. Chem.*, 2003, **68**, 1721; (*d*) D. Sloboda-Rozner, P. Witte, P. L. Alsters and R. Neumann, *Adv. Synth. Catal.*, 2004, **346**, 339; (*e*) D. Sloboda-Rozner, P. L. Alsters and R. Neumann, *J. Am. Chem. Soc.*, 2003, **125**, 5280; (*f*) A. Haimov and R. Neumann, *J. Am. Chem. Soc.*, 2006, **128**, 15697.
18 (*a*) H. Li, W. Qi, H. Sun, P. Li, Y. Yang and L. Wu, *Dyes Pigm.*, 2008, **79**, 105; (*b*) H. Li, P. Li, Y. Yang, W. Qi, H. Sun and L. Wu, *Macromol. Rapid Commun.*, 2008, **29**, 431.
19 X. Yan, P. Zhu, J. Fei and J. Li, *Adv. Mater.*, 2010, **22**, 1283.
20 (*a*) W. Adam, M. N. Korb, K. J. Roschmann and C. R. Saha-Möller, *J. Org. Chem.*, 1998, **63**, 3423; (*b*) A. Lattanzi, S. Piccirillo and A. Scettri, *Adv. Synth. Catal.*, 2007, **349**, 357.
21 J. Legros and C. Bolm, *Angew. Chem., Int. Ed.*, 2004, **43**, 4225.

